論文 / 著書情報
Article / Book Information

Title(English)	A generalized mean temperature difference method for thermal design of heat exchangers
Authors(English)	Utamura, M, Nikitin, K., Kato, Y.
Citation(English)	Int. national conf. on nuclear safety and education
Copyright	Copyright (c) 2007 Inderscience Publishing Co. Ltd.
発行日 / Pub. date	2007, 9
DOI	http://dx.doi.org/10.1504/IJNEST.2008.017545
URL	http://www.inderscienceonline.com/doi/abs/10.1504/IJNEST.2008.017545?journalCode=ijnest

A GENERALIZED MEAN TEMPERATURE DIFFERENCE METHOD FOR THERMAL DESIGN OF HEAT EXCHANGERS

Motoaki Utamura, Konstantin Nikitin and Yasuyoshi Kato

Tokyo Institute of Technology, 2-12-1 Ookayama Meguro-ku Tokyo 152-8552 Japan
tel +813-5734-3293, fax +813-5734-2959
E-mail utamura@rccre.titech.ac.jp

ABSTRACT

A generalized mean temperature difference (GMTD) method instead of logarithmic mean temperature difference (LMTD) method for heat exchangers is proposed. Unlike LMTD method, GMTD method allows performance analysis of heat exchangers with distributed physical properties. GMTD is calculated by a new method to take fluid temperature profiles as a function of heat load. Mathematical proof is made that the formula of LMTD can be derived from that of GMTD in the case of constant physical property. GMTD method is applied to experiments of a hot water supplier with supercritical carbon dioxide as a heating media that works through its pseudo critical point where specific heat behaves anomaly. The empirical correlations of local Nusselt number and pressure loss coefficient based on GMTD give accurate prediction of overall heat transfer coefficient with 5% error whilst two times larger error appears in the case of LMTD.

Key words: **logarithmic mean temperature difference method, generalized mean temperature difference method, overall heat transfer coefficient, super critical carbon dioxide, heat exchanger, Nusselt number**

NOMENCLATURE

A	Heat transfer area	[m^2]
a	Heat transfer area per unit length of heat exchanger	[m]
AOHTC	Averaged overall heat transfer coefficient	[W/m^{2}K]
C^*	Heat conductance ($=A_iU_i$)	[W/K]
Cp	Specific heat	[J/kgK]
D_h	Hydraulic diameter	[m]
F	Function(Eq.(22))	[W/m^{2}K]
f	Pressure loss coefficient	[-]
G	Mass flux	[kg/ m^{2}s]
GMTD	Generalized mean temperature difference	[K]
h	Specific enthalpy	[W/kg]
K	$= mCp$	
L	Length of heat exchanger	[m]
LMTD	Logarithmic mean temperature difference	[K]
MCHE	Microchannel heat exchanger	[-]
m	Mass flow rate	[kg/s]
N	Number of thermal unit(*NTU*)	[m]
Nu	Nusselt number($=\alpha D_h/\lambda$)	[-]
OHTC	Overall heat transfer coefficient	[W/m^{2}K]
ΔP	Pressure loss	[Pa]
Pr	Prandtl number	[-]
Q	Heat load	[W]
Re	Reynolds number ($=G D_h/\mu$)	[-]
s	Number of flow channel rows	[-]
T	Temperature	[K]
ΔT	Temperature difference between two fluids	[K]
Δt	Wall thickness	[m]
U	Overall heat transfer coefficient	[W/m^{2}K]
W	Mass flow of fluid	[kg/s]

Greek

α	Heat transfer coefficient	[W/m^{2}K]
λ	Heat conductivity	[W/mK]
μ	Viscosity of fluid	[Pa・s]
ρ	Fluid density	[kg/m^3]
Δ	Increment	

Subscript

i	Inlet, either 1(hot side) or 2(cold side)
o	Outlet
1	Hot side, Constant of Nusselt formula
2	Cold side, Constant of pressure loss coefficient

1. INTRODUCTION

Compactness and efficiency improvement of heat exchangers are important, particularly for cost reduction, in all energy system: heat pumps, refrigeration, and waste heat recovery systems for variety of residential, industrial, automotive and process industry applications. Logarithmic mean temperature difference (LMTD) method [1] has been a key concept to measure the compactness as shown in Colburn *j* factor, given as

$$j = \frac{D_h}{4L} Pr^{2/3} N \,, \tag{1}$$

where $N=NTU$ (Number of Thermal Units), and assuming $K_1 \le K_2$

$$N = (T_i^1 - T_o^1) / \Delta T_{LMTD} \,. \tag{2}$$

As shown in later chapter, the application of LMTD method is limited to a heat exchanger system containing fluid with constant physical property. Therefore ΔT_{LMTD} in Eq.(2) should be modified where physical property is not constant. On the other hand, as energy saving tactics and hence reduction of carbon dioxide emission in the air, super critical CO_2 cycle is likely to be adopted because of the advancement in turbomachinery technology [2]. For example electrically driven hot water suppliers tend to be widely introduced that use super critical CO_2 as a heating medium. It is because it has higher COP as well as non-toxic and non-artificial nature. The hot water supplier operates under the condition including pseudo critical point of CO_2. It is because thermodynamic

state of CO_2 is selected so as to minimize the work of compressor in the cycle. Physical properties there are quite sensitive to the temperature change and thus far much different from constant nature. Thus rigorous analysis of the performance of the hot water supplier requires the introduction of new methodology instead of LMTD method. The purpose of this study is to derive a generalized mean temperature difference (GMTD) method and show its validity by applying experiment of hot water supplier using super critical CO_2 and water as heating media.

2. THEORY

2.1 Derivation and limitation of log mean temperature difference method

For counter-flow heat exchangers in Fig.1, temperature profiles of two fluids obey the following governing equations

$$m_1 Cp_1(x)\frac{dT_1}{dx} = -a_1 U_1(x)(T_1 - T_2)$$
$$m_2 Cp_2(x)\frac{dT_2}{dx} = -a_2 U_2(x)(T_1 - T_2)$$
where (3)
$$a_1 U_1(x) = a_2 U_2(x) = c(x)$$
$$a_i = A_i / L$$

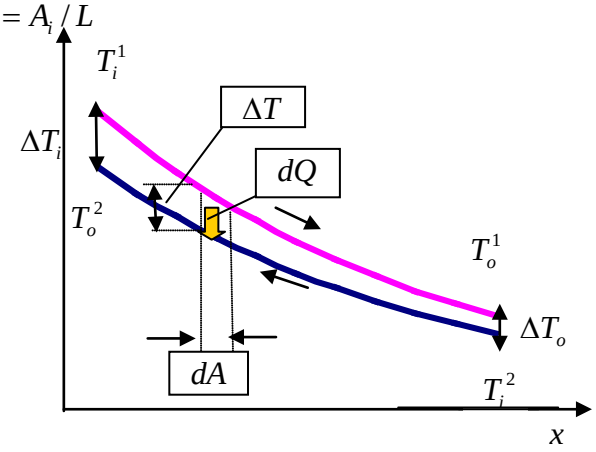

Fig.1 Variation of the fluid temperatures in a counter-flow heat exchanger

For parallel-flow configuration m_2 should be replaced by $-m_2$. From Eq. (3) following equation can be reduced

$$K_1(x)K_2(x)\frac{d\Delta T}{dx} = c(x)(K_1(x) - K_2(x))\Delta T(x)$$
where (4)
$$\Delta T(x) = T_1(x) - T_2(x)$$
$$K_i(x) = m_i Cp_i(x)$$

Provided K_i, c are constants, analytical integration of Eq.(4) can be executed, yielding to

$$\Delta T(x) = \Delta T_i e^{\gamma x}$$
and
$$\Delta T_o = \Delta T_i e^{\gamma L}$$
where (5)
$$\gamma \equiv c\left(\frac{1}{K_2} - \frac{1}{K_1}\right)$$
$$K_i = m_i Cp_i$$

Noting

$$Q_0 = K_1(T_1^i - T_1^o) = K_2(T_2^0 - T_2^i)$$
Then (6)
$$\Delta T_o - \Delta T_i = Q_0\left(\frac{1}{K_2} - \frac{1}{K_1}\right) = \frac{\gamma Q_0}{c}$$

From Eqs.(5) and (6)

$$ln\frac{\Delta T_o}{\Delta T_i} = \gamma L = \frac{C^*}{Q_0}(\Delta T_o - \Delta T_i) \quad (7)$$

If we define ΔT_{LMTD} as

$$\Delta T_{LMTD} = \frac{\Delta T_o - \Delta T_i}{ln\frac{\Delta T_o}{\Delta T_i}} \quad (8)$$

From Eq.(7) we have

$$Q_0 = A_i U_i \Delta T_{LMTD} = C^* \Delta T_{LMTD} \quad (9)$$

For example by use of Eq.(9) one could obtain an overall heat transfer coefficient (OHTC) U_i from measurements.

2.2 Temperature difference as function of heat load Q

For an infinitesimal segment of a heat exchanger, following equation holds

$$dQ = U_i dA_i \Delta T$$
$$dA_i = \frac{A_i}{L}dx \quad (10)$$

In the case of constant physical properties, using temperature difference between fluids at both ends, Eq.(5) can be alternatively expressed by

$$\Delta T = \Delta T_i e^{\frac{x}{L} ln\frac{\Delta T_o}{\Delta T_i}} \quad (5)'$$

Integration of Eq.(10) using Eq.(5)' gives the relation between heat load Q and length x as

$$Q = \frac{c\Delta T_i}{ln\dfrac{\Delta T_o}{\Delta T_i}}\left(e^{\frac{x}{L} ln\frac{\Delta T_o}{\Delta T_i}} - 1 \right) \tag{11}$$

at $x = L$

$$\frac{\Delta T_o}{\Delta T_i} = \frac{ln\dfrac{\Delta T_o}{\Delta T_i}}{c\Delta T_i} Q_0 + 1 \tag{12}$$

By use of Eq.(12), Eq.(11) can be rewritten as

$$\frac{Q}{Q_0} = \frac{e^{\frac{x}{L} ln\frac{\Delta T_o}{\Delta T_i}} - 1}{\dfrac{\Delta T_o}{\Delta T_i} - 1} \tag{11'}$$

Application of Eq.(11)' to Eq.(5)' gives for ΔT as function of Q

$$\Delta T = \Delta T_i \left[\left(\frac{\Delta T_o}{\Delta T_i} - 1 \right) \frac{Q}{Q_0} + 1 \right] \tag{13}$$

It is seen ΔT is a linear function of Q in the case of constant physical properties.

2.3 Generalized mean temperature difference (GMTD) method for variable physical properties

Integration of Eq.(10) over an entire heat exchanger gives

$$\int_0^{Q_0} \frac{dQ}{\Delta T(Q)} = \int_0^{A_i} U_i dA_i \tag{14}$$

If we define generalized mean temperature difference $\Delta \overline{T}$ and averaged overall heat transfer coefficient $\overline{U}_i$ by

$$\begin{aligned} \frac{1}{\Delta \overline{T}} &\equiv \frac{1}{Q_0} \int_0^{Q_0} \frac{dQ}{\Delta T(Q)} \\ \overline{U}_i &\equiv \frac{1}{A_i} \int_0^{A_i} U_i dA_i \end{aligned} \tag{15}$$

then similar to Eq.(9), from Eq.(14) we have

$$Q_0 = A_i \overline{U}_i \Delta \overline{T} = \overline{C}^* \Delta \overline{T} \tag{16}$$

Provided $Q_0, A_i, \Delta \overline{T}$ in prior for example from experiments or design condition, Eq.(16) gives an averaged overall heat transfer coefficient (AOHTC) $\overline{U}_i$. Also, with $Q_0, \overline{U}_i, \Delta \overline{T}$ given one can determine heat transfer area A_i and the size of the heat exchanger. Eq.(2) may also be modified as

$$N = (T_i^1 - T_o^1) / \Delta \overline{T} \tag{2'}$$

One can execute numerical integration of the first equation of Eq.(15) and evaluate $\Delta \overline{T}$ provided heat duty Q_0 and inlet temperatures T_i^1 and T_i^2 of both fluids is given. In the case that U_i is constant, clearly $\overline{U}_i$ and $\Delta \overline{T}$ are exactly equal to U_i and ΔT_{LMTD} respectively as follows.

Using Eq.(15)

$$\begin{aligned} \frac{1}{\Delta \overline{T}} &= \frac{1}{Q_0} \int_0^{Q_0} \frac{dQ}{\Delta T(Q)} \\ &= \frac{1}{\Delta T_i} \frac{1}{\dfrac{\Delta T_o}{\Delta T_i} - 1} ln \left[\left(\frac{\Delta T_o}{\Delta T_i} - 1 \right) \frac{Q}{Q_0} + 1 \right]_0^{Q_0} \end{aligned} \tag{17}$$

This leads to

$$\Delta \overline{T} = \frac{\Delta T_o - \Delta T_i}{ln\dfrac{\Delta T_o}{\Delta T_i}} = \Delta T_{LMTD} \tag{18}$$

3. NUMERICAL CALCULATION

3.1 Numerical procedure

Given $Q_0, T_i^1, T_i^2, m_1, m_2, P_i^1$ and P_i^2, temperature profiles of both fluids and resultant temperature difference profile may be obtained as follows. Calculating specific enthalpies at inlets one can obtain specific enthalpy and temperature of cold side fluid (indicating by suffix 2) at outlet. Next, heat duty Q_0 is expressed by a sum of M sets of heat segment $q(=Q/M)$ each of which is sequentially numbered from the hot side fluid entry.

Calculation starts from the first segment. Enthalpies and temperatures at the node on the right edge of the segment are obtained from heat balance and thermodynamic state equation. Thermodynamic state of each fluid was calculated by PROPATH [3] in this study. As the node on the right edge of the segment shares the node on the left edge of the next segment, calculation proceeds in sequence until heat load reaches the heat duty given. At each node temperature difference of two fluids is calculated. Thus

$$\int_0^{Q_0} \frac{dQ}{\Delta T(Q)} = \sum_{j=1}^{M} 2q / (\Delta T_j + \Delta T_{j+1}) \tag{19}$$

and

$$\Delta \overline{T} = M \Big/ \sum_{j=1}^{M} 2 / (\Delta T_j + \Delta T_{j+1}) \tag{20}$$

3.2 Numerical example

3.2.1 Constant physical property

Fig.2 shows temperature difference profile using Eq.(13) with $\Delta T_i = 28$, $\Delta T_o = 9$, $Q_0 = 4.6kW$ under constant physical property. Mean temperature difference by LMTD method gives 16.7K and pinch point appears at the entry of cold fluid.

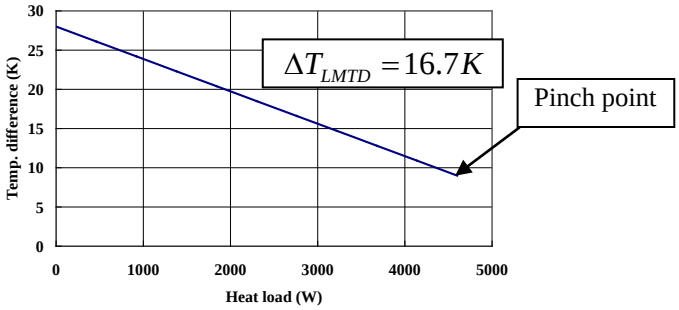

Fig.2 Temperature difference profile under constant physical property

3.2.2 Distributed physical property

With the same inputs as above, pseudo critical state of carbon dioxide and water were considered as heating media. Figs. 3, 4 and 5 show physical property variations, temperature profile and a variation of temperature difference between two fluids expected in hot water suppliers. Physical properties were calculated by PROPATH [3]. Pinch point appears in the middle of the heat exchanger where specific heat has a maximum at pseudo critical point of carbon dioxide. Critical point exists at 7.4MPa and 303K. Eq.(20) gives $\Delta\overline{T}$ =9.6K being 58% of ΔT_{LMTD} =16.7K due to non-linear characteristics of physical properties. Averaged heat conductance $\overline{C}^*$ was evaluated to be 480W/K.

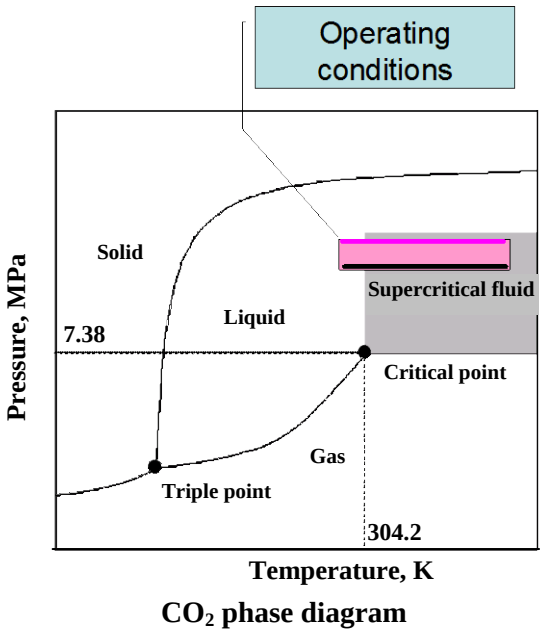

Fig.3 Behavior of physical property of carbon dioxide in pseudo critical state

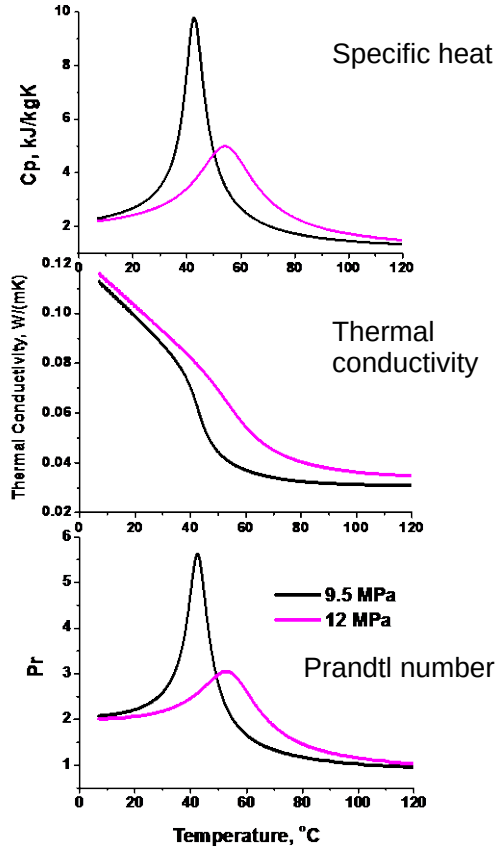

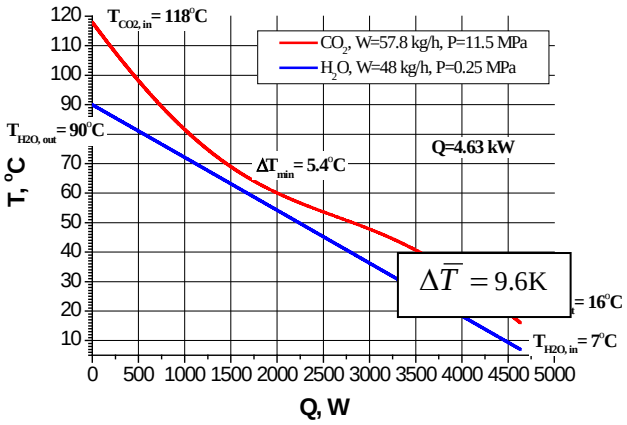

Fig.4 Temperature profile in heat exchanger with distributed physical property

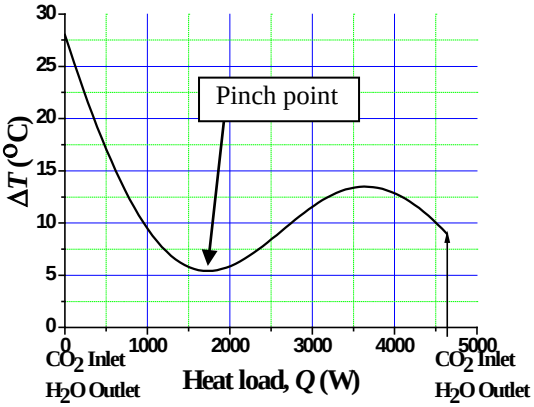

Fig.5 Temperature difference profile reduced from Fig.4

This implies 1/0.58=1.73 times larger heat transfer area than those predicted by LMTD method is actually needed, which differentiates between the present methodology and LMTD method.

3.2.3 Limitation of heat exchange rate

In terms of temperature profile as function of heat load, Fig.6 shows an example of impossible temperature profile in practice. This method in turn shows where the limitation of heat exchange capacity is and suggests countermeasures for it. With given flow rates 17degC of inlet water temperature cannot produce hot water of 65 deg C. It comes from huge specific heat of carbon dioxide at the state quite near the critical pressure (P=7.4MPa see Fig.3). Analysis indicates an inlet water temperature of 54deg C at least should be prepared to obtain hot water of 65 degC at exit and a resultant heat duty available will be limited to 1500W where temperature difference between two fluids becomes zero. Thus, owing to the method an operable range could be known without physical dimensions and OHTC. Thus design heat duty of 6.02kW is not attainable under the pressure condition of 8MPa.

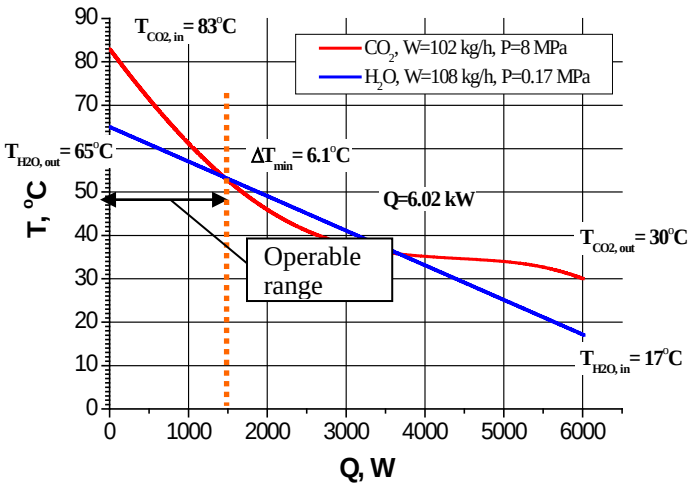

Fig.6 Operability and heat exchange capability

4. VERIFICATION BY EXPERIMENT

In order to demonstrate the validity of the present methodology (GMTD), experiments were carried out to derive empirical correlations for Nusselt number and pressure loss factor for hot water suppliers using super critical carbon dioxide and water as heating media.

4.1 Experimental facility

A schematic diagram of the experimental loop is shown in Fig. 7. Carbon dioxide from the low pressure tank is compressed by the oil compressor. High-pressure gas is heated by an electric heater 1 (1.9 kW) before passing through gas cooler 1 and after the oil separators. The resulting CO_2 is forwarded through a turbine type flow meter to the inlet of the test section where microchannel heat exchanger (MCHE) is installed. The description of MCHE can be found elsewhere[4].The pressure of CO_2 gas discharged from the MCHE outlet is reduced by a flow rate control expansion valve and transferred to an electric heater 2 (2.2 kW). CO_2 gas is heated by an electric heater 2 (2.2 kW) in order to maintain the CO_2 in gas phase. Because of adiabatic expansion process, the pressure of CO_2 is lowered, so the temperature becomes saturated temperature. After heating by heater 2, CO_2 gas temperature is adjusted by the gas cooler 2 to obtain a suitable CO_2 gas temperature before returning to the CO_2 low pressure tank. The flow meter of the CO_2 side is installed just after gas cooler 2. The city water is directly supplied to the H_2O side inlet; the city water temperature can be adjusted using the chiller/warmer to meet the required testing conditions.

Experimental procedure is as follows. While water inlet pressure is not controlled (~0.2-0.3MPa), CO_2 inlet pressure is controlled by compressor and bypass valve. CO_2 inlet temperature is controlled by Heater 1 and Cooler 1 while water inlet temperature by additional heater/cooler (not shown). Water outlet temperature is controlled by water flow rate control system (not shown). CO_2 flow rate is controlled by CO_2 flow rate control system (not shown). Only CO_2 flow rate is varied during experiment. Water flow rate is obtained as a result of water outlet temperature control.

The experimental facility requires about 3 hours reaching a steady state condition from the beginning of an experimental run. When some parameters are changed (e.g. a flow rate) it requires 30 minutes to approach a new steady state condition. A steady state condition was determined as a condition when the fluctuation of measured parameters is well within the range of measurement accuracy for at least 10 minutes. The CO_2 and H_2O temperatures, pressures and pressure drops were directly measured and used in the further calculations while the flow rate value was corrected according to the measured CO_2 temperature and pressure near the location of the flow meter. The corrective dependencies were provided by the manufacturer of the experimental loop. All the values were then averaged over 5 minute intervals. Throughout the day of the experiment the inlet pressure and temperature of hot/cold side were kept constant while the set value of the flow rate was changed in 5 kg/h increments.

The MCHE was manufactured from three flat copper plates that have fluid flow passages chemically milled into them. This technique is similar to that used in the manufacture of electronic printed circuit boards. The plates are then diffusion bonded together into blocks to form a heat exchanger core of the required capacity.

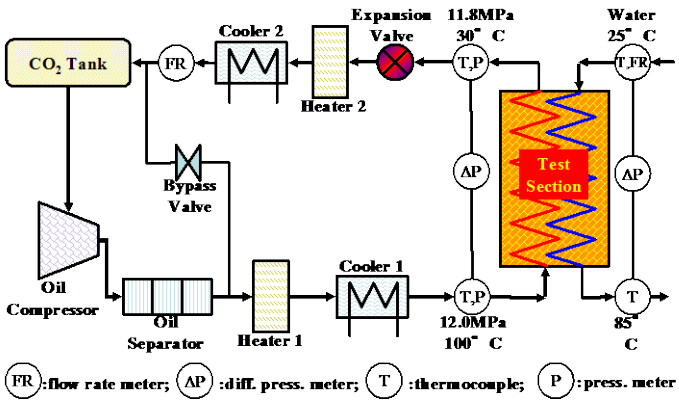

Fig.7 Flow diagram of supercritical CO_2 experimental loop

The new MCHE has core dimensions of 870×78×14mm as shown in Fig.8. This MCHE includes two CO_2 and one H_2O plates combined in sandwich structure, so-called double banking. Hot side and cold side fluid are CO_2 and water respectively. Flow direction of fluids is countercurrent.

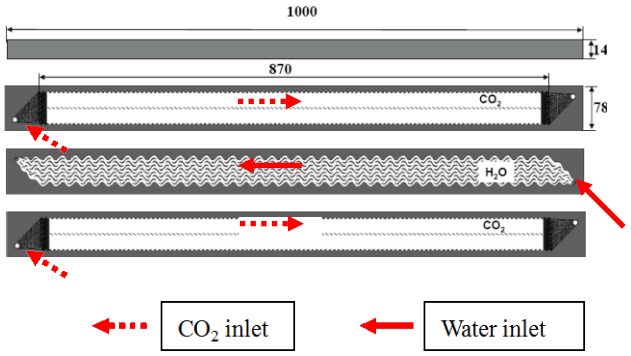

Fig.8 Configuration of microchannel heat exchanger

4.2 Instrumentation

The CO_2 inlet pressure of the MCHE was measured using a pressure gauge transducer with an accuracy of ±0.25% over the full range of 13 MPa. The pressure drop was measured using a differential pressure gauge with an accuracy of ±0.15% over the full range of 400 kPa for the CO_2 side and 50 kPa for H_2O side. The T-type (Copper/Constantan) thermocouples with accuracy of ±0.5°C at the range of 40–125°C were used for temperature measurement in both cold and hot side. Thermocouples were inserted into the inlet and outlet of MCHE's distributors. All thermocouples were calibrated at a water boiling and ice point. The CO_2 flow meter accuracy was ±5% over the full range of 20–88 kg/h.
All measurements were recorded automatically with a 0.5-Hz sampling frequency.

4.3 Experimental conditions

The inlet temperature of CO_2 side is set at about 100° C and 118° C while the pressure reach up to 11.0 to 12.5 MPa. This hot super critical CO_2 heat up the city water from 7° C or 25° C to 85° C, 90° C or 95° C throughout the new MCHE or double tube heat exchanger. The city water's pressure is estimated circa 0.25 MPa. The outlet temperature of CO_2 side or the flow rate of H_2O is the dependent parameter resulting from heat exchange in test sections. More than fifty test cases were run. Those experimental conditions are clearly given in Table 1. It should be noted that both Reynolds number and Prandtl number varies not only among test runs but also within the heat exchanger.

Table 1 Experimental conditions

		CO_2 side		Water side	
		min	max	min	max
Press. (MPa)		9.5	12.6	~0.25	
Flow rate(kg/h)		26.8	81.1	17.4	50.4
Temp.(deg C)	inlet	99.2	120.4	4.3	27.6
	outlet	19.4	45.6	84.9	93.4
Heat load(W)		1604	4628	1604	4628
Reynolds No.	Inlet	7351	19773	110	587
	Outlet	1832	9960	510	1627
Prandtl No.	Inlet	1.03	1.05	5.74	11.43
	Outlet	2.06	2.89	1.89	2.10

4.4 Correlation for Nusselt number

An empirical formula of local Nusselt number was obtained based on GMTD method.

Two assumptions were made;

1) The same equation can be applied to both fluids. It is because the central part of the flow channel of MCHE is geometrically similar between both flow channels.
2) It is possible to express the Nusselt number as the product of polynomials of Reynolds and Prandtl number as

$$Nu = C_1 \times Re^m Pr^n \tag{21}$$

Heat conductance may be expressed by

$$C^* = U_2 A_2 = 1 \Big/ \left(\frac{1}{\alpha_1 A_1} + \frac{\Delta t_w}{\lambda A_w} + \frac{1}{\alpha_2 A_2}\right) \tag{22}$$

,where heat transfer coefficient α is related to Nu as $\alpha = \frac{\lambda Nu}{D_h}$ from the definition of Nusselt number.

In Eq.(22) the product of $\Delta t_w / \lambda A_w$ is one hundred times less than the other terms and was neglected since the conductivity of copper is 387W/(mK) with the wall thickness of MCHE is about o.5mm. Then, by substituting Eq.(21) into Eq.(22) and using the assumption 1), we have

$$U_2 = \frac{C_1 A_1 \lambda_2 \lambda_1 Re_1^m Pr_1^n Re_2^m Pr_2^n}{D_h^1 A_2 \lambda_2 Re_2^m Pr_2^n + D_h^2 A_1 \lambda_1 Re_1^m Pr_1^n} \equiv C_1 F \tag{23}$$

Note that C_1 is common to that of Eq.(21). Local physical properties, F and U_2 can be calculated based on local bulk temperature and pressure of fluid. To this end they should be functions of heat load. Using Eqs.(15) and (23), the calculation of averaged overall heat transfer coefficient (AOHTC) was numerically executed by change in variables

$$\bar{U}_i^{calc.} = \frac{1}{A_i}\int U_i dA_i = \frac{1}{A_i}\int U_i(Q)\frac{dA_i}{dQ}dQ \cong \frac{1}{Q_0}\int U_i(Q)\frac{\Delta \bar{T}}{\Delta T(Q)}dQ = \frac{C_1}{M}\sum_{j=1}^{M} F_j \frac{\Delta \bar{T}}{\Delta T_j} \equiv C_1 \bar{F} \tag{24}$$

Provided power indices m and n *in* Eq.(21) are determined in prior, then $\bar{F}$ can be calculated and constant C_1 may be obtained by application of least square method. Determination of m and n should be referred to [5]. The number of sub-divisions M of the heat exchanger was typically one thousand. It is important to note that thermal parameters should be expressed by heat load in order to evaluate local properties.

4.5 Pressure loss coefficient

Pressure loss behavior is closely related to heat transfer characteristics in the case of variable physical properties. Once correlation for Nusselt number is obtained, then with the help of Eq.(10), pressure loss may be numerically calculated

by the change of independent variable from length to heat load as

$$\Delta P = \int_0^L \varphi dx = \int_0^{Q_0} \varphi \frac{dx}{dQ} dQ = \int_0^{Q_0} \varphi \frac{dQ}{c\Delta T} \qquad (25)$$

$$\varphi \equiv fG^2 / 2\rho D_h$$

Here, functional form of $f = C_2 Re^{-r}$ was assumed for CO_2 side. C_2 and r were best fitted against pressure drop measurements by means of least square method. Thus, hydraulic characteristics are closely connected to thermal characteristics in a heat exchange system of variable physical property.

5. DISCUSSIONS

5.1 Thermal performance

5.1.1 Comparison of GMTD method with LMTD method

Literatures show power index of Reynolds number 0.8 is applicable to a variety of fluids.
Parametric study was done for power index of Prandtl number ranging from 0 to 0.8. It is found that $Pr^{0.6}$ gives the best fit to FLUENT calculation for MCHE. Therefore, the Nusselt number formula finally can be obtained in the following form:

$$Nu = C_1 \times Re^{0.8} Pr^{0.6} \qquad (26)$$

Fig.9 shows the results. The axis shows measured $\overline{U}_i$(AOHTC) reduced by Eq.(16) and abscissa calculated by Eqs.(23) and (26). Both were based on hot side (carbon dioxide side) heat transfer area. As a whole data are well correlated in line and the assumption 1) in section 4.4 was proved. Best fitted value of C_1 for PCHE-M(MCHE) gives C_1=0.0473 in Eq.(26). Prediction error by the present correlation applied to MCHE was 5%. Shown in Fig.10 regarding mean temperature difference, LMTD is ~2 times larger than GMTD. This implies LMTD may give smaller heat transfer area in the present case. Fig.11 shows averaged heat conductance. It is clearly demonstrated that GMTD method gives an excellent correlation with a small prediction error while LMTD method gives a poor result.

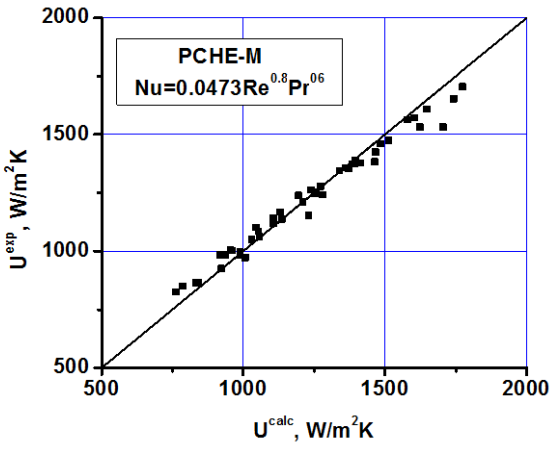

Fig. 9 Relation of $\overline{U}^{exp.}$ and $\overline{F}$

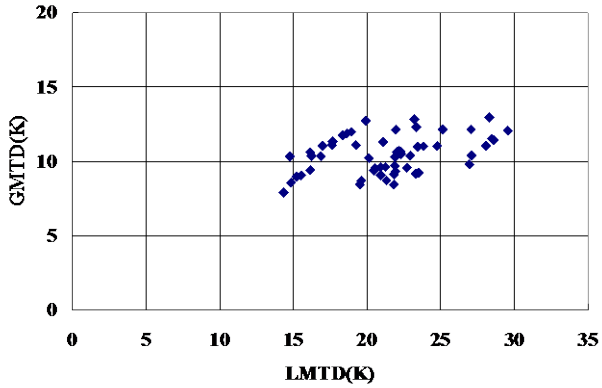

Fig. 10 Comparison of GMTD and LMTD

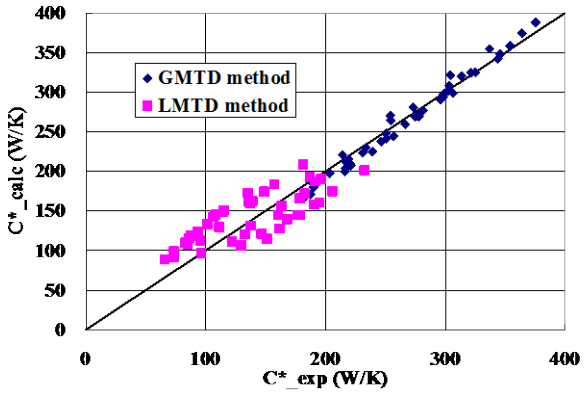

Fig.11 Heat conductance by two methods

5.1.2 Comparison of reproduced temperature with measured one

Fig. 12 compares measured temperatures along heat exchanger length with reproduced temperature profile using Eq.(26) with C_1=0.0473. Cold means water and hot means CO_2. Excellent agreement was obtained in the entire region of MCHE. Length was calculated by applying overall heat transfer coefficient and heat transfer area per length step by step in heat load segment. Four data plots at right and left ends of two curves exhibit fluid temperatures measured at inlet and exit plenums whose locations are indicated by red arrows in Fig.8. Similarly Fig.13 exhibits calculated profiles of overall heat transfer coefficient and heat transfer coefficient of both fluids. Significant profiles of heat transfer coefficients were observed as anticipated. It is also seen heat transfer rate is governed by water side heat transfer coefficient which comes from bigger hydraulic diameter of channel. Also overall heat transfer coefficient U is seen to have a large distribution in the heat exchanger tested.

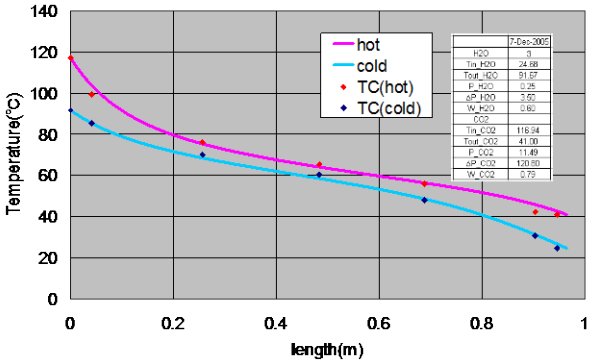

Fig. 12 Predicted and measured temperature profile in MCHE

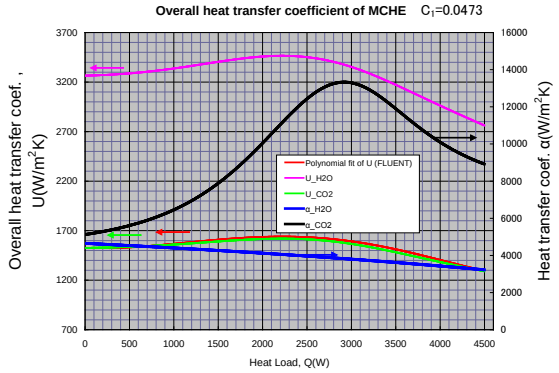

Fig. 13 Calculated profile of OHTC and HTC in MCHE

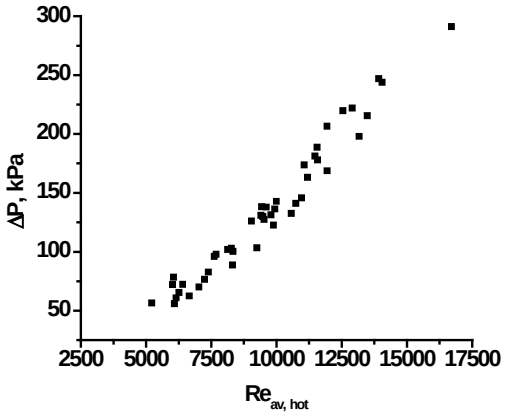

Fig. 14 Pressure loss correlated with averaged *Re*

5.2 Hydraulic performance

From COP (coefficient of performance) point of view, pressure drop in CO_2 side is important. Fig.14 attempts to correlate pressure loss measured at hot side in terms of Reynolds number averaged over an entire heat exchanger (MCHE). Data are seen scattered. It is due to the fact that Reynolds number also has a big profile in the heat exchanger caused by the variation of dynamic viscosity. Next with the help of Eq.(25) where local pressure loss influenced by heat transfer effect was taken into account, parametric studies were carried out. Functional form of pressure loss coefficient $f = C_2 Re^{-r}$ was assumed and unknown parameters C_2 and r were determined so that calculation fit measured data best. Fig.15 shows the result with C_2=2.294 and r=0.25. Excellent prediction was obtained unlike Fig.14. Prediction error was within 5% for MCHE. This is because local heat transfer effect i.e. the distribution of the product of $c\Delta T$ is taken into account in Eq.(25). Coincidently the same value of power as Blasius formula was obtained.

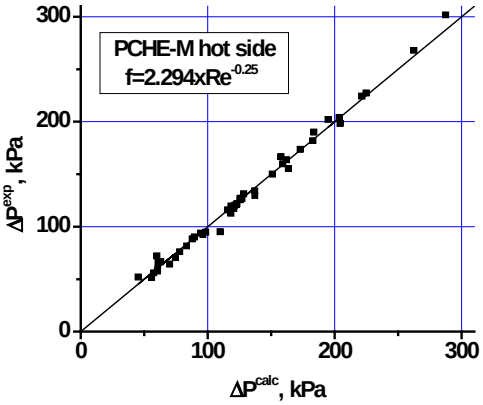

Fig. 15 Comparison of calculation with experiment

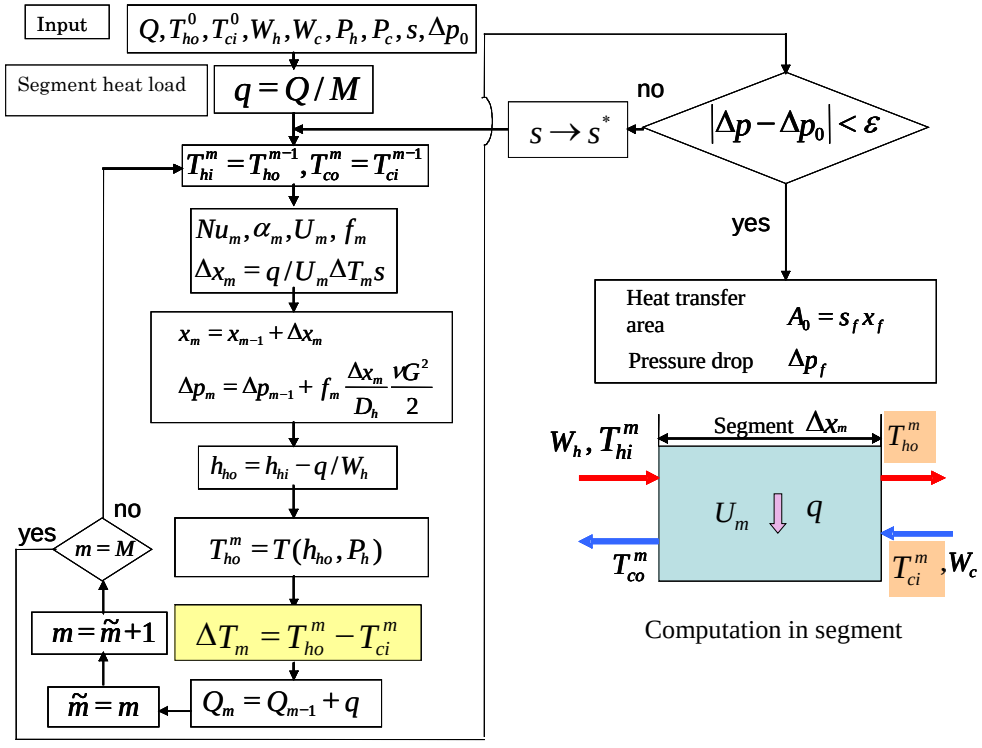

Computation in segment

Fig.16 Design flow diagram for heat exchangers with distributed physical properties

5.3 Design flow diagram using GMTD method

Design flow diagram for heat exchangers with variable physical properties is shown in Fig.16. For a given heat duty ,inlet conditions, mass flow rates and pressures heat exchanger length and width is obtained so as to keep pressure loss at specified value. Length Δx_m of heat load segment m is calculated using overall heat transfer coefficient derived from local Nusselt number (Eq.(26)) and incremental pressure loss is calculated in a similar way. After convergence heat transfer area as well as length will be obtained.

5. CONCLUSIONS

Generalized mean temperature difference (GMTD) method was proposed for thermal-hydraulic analysis of heat exchangers with distributed physical properties. This method gives exactly the same result as logarithmic mean temperature difference (LMTD) method in the case that physical properties are all constant. For the case of hot water supplier operating with super critical carbon dioxide as heating media GMTD was calculated, which is about 0.6 times less than LMTD. Moreover experimental validation of the methodology was carried out using super critical CO_2 test loop. Empirical formulae for local Nusselt number and local pressure loss factor were obtained using GMTD method. Reproduction of temperature profiles was compared with measurements, in which excellent agreement was obtained. Based on the correlation developed design flow diagram was also developed for heat exchangers with distributed physical properties. In the case OHTC is given direct usage of LMTD method was found to predict smaller heat transfer area of heat exchangers with distributed physical properties in the present operating conditions. Therefore we can safely conclude that LMTD method may be substituted by the present GMTD method for the design of heat exchangers in general, in particular suitable for the case where distributed physical properties are anticipated.

ACKNOWLEDGEMENT

Work partly performed under the program of “Strategic development of Technology for Efficient Energy Utilization-Project of Fundamental Technology Development for Energy Conservation” sponsored by NEDO.

REFERENCES

[1] Hesselgreaves, J. E., 2001.”Compact Heat Exchangers, Selection, Design and Operation”, pp. 1-2, Pergamon.
[2] Utamura,M. and Tamaura,Y.,2006,”A Solar Gas Turbine Cycle with Super-Critical Carbon Dioxide as a Working Fluid”, Proc. ASME TURBO EXPO 2006, GT2006-90864,May 8-11,Barcelona,Spain.
[3] Ito, T., et al.,1990, PROPATH: A Program Package for Thermo-physical Properties of Fluids, Version 10.2, Corona Publishing Co., Tokyo, Japan.
[4] Tsuzuki, N., Kato, Y., Ishiduka, T. 2005, “High performance printed circuit heat exchanger,” Heat SET 2005, Heat Transfer in Components and Systems for Sustainable Energy Technologies, April 5–7, Grenoble, France.
[5] Utamura,M., Kato,Y., Nikitin, K., Ngo, T., L. and Ishizuka,T., 2006,“Empirical Correlations for Thermal-Hydraulic Characteristics of Compact Heat Exchangers with Microchannels”, NTHAS5-N001, Proc. 5th Korea-Japan Symposium on Nuclear Thermal Hydraulics and Safety, November 26–29, Jeju, Korea.